JOURNAL OF Materials CHEMISTRY

Organogels are useful as a template for the preparation of novel helical silica fibers

Yoshiyuki Ono,[a] Kazuaki Nakashima,[a] Masahito Sano,[a] Junichi Hojo[b] and Seiji Shinkai*[a,b]

[a]*Chemotransfiguration Project, Japan Science and Technology Corporation (JST), 2432 Aikawa, Kurume, Fukuoka 839-0861, Japan*
[b]*Department of Chemistry and Biochemistry, Graduate School of Engineering, Kyushu University, Hakozaki, Higashi-ku, Fukuoka 812-8581, Japan.*
E-mail: seijitcm@mbox.nc.kyushu-u.ac.jp; Fax: +81-942-39-9012; Tel: +81-942-39-9011

Received 19th March 2001, Accepted 19th June 2001
First published as an Advance Article on the web 8th August 2001

Sol–gel polymerization of tetraethoxysilane (TEOS) was carried out in the organogel phase consisting of cholesterol-based gelators (neutral **1** and cationic **2**). TEOS polymerization in neutral **1** + $MeCO_2H$ gel resulted in the conventional granular silica whereas that in cationic **2** + $MeCO_2H$ gel yielded the novel mesoporous silica with a tubular structure. SEM and TEM observations and additive effects established that the organogel fibers act as a template in the TEOS polymerization process to yield the hollow silica fibers and that the electrostatic interaction plays a crucial role in adsorption of anionic oligomeric silica particles onto the cationic organogel fiber surface. Thus, the tubular structure is created after combustion of the gelators by calcination. Very interestingly, when TEOS polymerization was carried out in the **1** + **2** mixed organogel, fibrous silica with a right-handed "helical" structure was created. This phenomenon appeared only in the range of **2**/(**1** + **2**) = 5–15 mol%. Since the higher-order helical structure is characteristic of supramolecular assemblies of "chiral" organic compounds, it is suggested that the chirality in the organogel fibers is successfully transcribed into the inorganic silica fibers. Thus, the concept presented in this paper describes a novel template effect and should be broadly applicable to the design of "supramolecular" silica materials useful for catalysts, memory storage, replication, *etc.*

Introduction

A diversity of supramolecular structures can be created, not only in Nature but also in an artificial system, by self-assembly of designed organic building blocks. In general, creation of such diverse supramolecular structures seems to be very difficult or nearly impossible in inorganic materials. Is there any innovative method by which inorganic materials can be self-assembled into the ordered supramolecular structures? The sole method which can satisfy this requirement would be, if any, to transcribe the supramolecular structures of organic molecular assemblies into inorganic materials.

It is known that amphiphilic organic molecules are self-assembled into various supramolecular structures.[1] These self-assemblies can be utilized as a template to create novel mesophasic inorganic materials in mesoporous materials,[2] vesicles,[3] ultra-thin membranes,[4] *etc.*[5] These phenomena have attracted chemists not only for the development of new inorganic materials but also as biomimetic processes of biomineralization. As natural examples for these processes, one can raise inorganic micro-fibers prepared by mineralization of bacterial fibers[6] or of self-assembled lipid tubules of a galactocerebroside and a phosphate.[7] These attempts are very important as guidelines for the "design" of the shapes and sizes of inorganic materials (analogous to "design" strategies for organic assemblies).[8] A similar technique on a μm level has already been applied to the preparations of catalysts, electro-devices, *etc.*[9]

Increasing attention has been paid to low molecular-mass compounds that can efficiently gelate various organic solvents.[10–21] These phenomena are interesting in that the fibrous aggregates formed by noncovalent interactions are responsible for the gelation. In particular, cholesterol-based gelators (*e.g.*, **1**), which can form stable gels using only non-hydrogen-bonding interactions, show an excellent gelation ability towards a wide variety of organic solvents at low concentrations.[14–18,20,21] In addition, the resulting gels have chirally-oriented structures which are imparted from the characteristic cholesterol skeleton.[16] Through these studies we found that even liquid silanol derivatives can be gelated by some cholesterol-based gelators.[16,22] It thus occurred to us that if sol–gel polymerization of silanol derivatives proceeds in the organogel phase, the gelator fibrils should act as a template which eventually creates a void in the resultant silica. After trial-and-error, we have found that under the limited reaction conditions a cholesterol-based "cationic" gelator (**2**) which can gelate a tetraethoxysilane (TEOS) solution acts as an efficient template in sol–gel polymerization to give a novel mesoporous silica with a tubular, macaroni-like structure. Furthermore, we have found that when **1** and **2** are mixed in a specific molar ratio, the resultant organogel system yields the very unique, right-handed "helical" silica. These novel findings consistently support the view that sol–gel polymerization in the organogel system is an efficient and versatile method to create novel silica super-structures,[22,23] because organic gelators form variable structures not only in size but also in shape. It is very interesting that the helical structures in the silica fiber are created by the template which apparently shows no helical structure.[23]

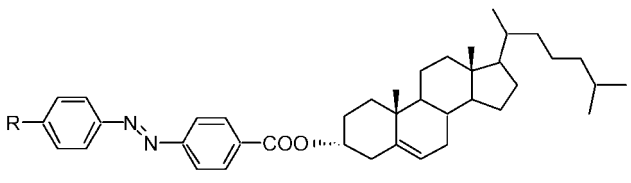

1: R=$O(CH_2)_2Me$
2: R=$O(CH_2)_4NMe_3^+Br^-$

 DOI: 10.1039/b102550n

Experimental

Syntheses

The synthesis of **1** was described previously.[16] Compound **2** was synthesized according to Scheme 1. A mixture of *p*-[*p*-(4-bromobutoxy)phenylazo]benzoic acid[24] (**3**: 2.60 g, 6.91 mmol), triphenylphosphine (4.77 g, 18.2 mmol), cholesterol (2.67 g, 6.91 mmol), and azodicarboxylic acid diethyl ester (6.29 g, 36.1 mmol) in THF (104 ml) was stirred at room temperature for 3 days. The solution was evaporated to dryness, the resultant product being subjected to purification by silica column chromatography. The product (**4**) was used for the next reaction without further purification. A THF solution (25 ml) containing **4** (0.62 g, 0.91 mmol) was cooled in a dry ice–methanol bath. To this solution was introduced trimethylamine gas from the aqueous trimethylamine solution (5.38 g, 91 mmol). The quaternization reaction was continued for 18 h: yield 8.6%; ^{1}H NMR ($CDCl_3$, 300 MHz) δ 0.60–2.70 (m, 47H, cholesterol and -CH_2-CH_2-), 3.48 (s, 9H, $(CH_3)_3N$), 3.81–3.84 (t, 2H, NCH_2), 4.16–4.17 (t, 2H, CH_2O), 5.28–5.34 (m, 2H, cholesterol 3-H and 6-H), 7.01–7.04 (d, 2H, ArH), 7.88–8.14 (m, 6H, ArH); IR (KBr) 1711 ($\nu_{C=O}$) cm^{-1}; Anal. Calcd for $C_{47}H_{70}O_3N_3Br.H_2O$: C, 68.59; H, 8.82; N, 5.11. Found: C, 68.89; H, 8.76; N, 5.08; MS (positive SIMS, NBA) *m*/*z* 724 [M$^+$]. Since triphenylphosphine and azodicarboxylic acid diethyl ester were used for the condensation with cholesterol (with (*S*)-configuration for C-3), the absolute configuration of the C-3 carbon is inverted to (*R*)-configuration.[16,25] This is confirmed by the ^{1}H NMR spectra of **1** and **2**. In **1** and **2**, the peaks of cholesterol 3-H and 6-H overlap and appear at 5.20–5.40 ppm for **1** and 5.28–5.34 ppm for **2**, respectively. On the other hand, in a stereoisomer of **1** in which C-3 adopts the (*S*)-configuration cholesterol 3-H and 6-H appear separately (at 4.80–5.20 ppm for 3-H and 5.50–5.60 ppm for 6-H, respectively).

Gelation test

The gelator and the solvent were put in a septum-capped test tube and the solution was heated until the solid was dissolved. The solution was cooled in ice–water to *ca.* 4 °C. When the solvent was entirely gelated, it was warmed to ambient temperature by air or water. If the gel was stable, it was classified as "G" in Table 1. The mark "SG" denotes that the gel is formed at the concentration of a gelator **2** lower than 1.0 wt%. When the solvent was not gelated, it was cooled in a refrigerator (−6 °C). If the gel was formed only in the refrigerator, it was classified as "Gf"' in Table 2. "S" denotes that the gel is not formed because of high solubility whereas "I" denotes that the solid is insoluble even in the refluxing solvent.

Sol–gel polymerization conditions

Sol–gel polymerization was carried out as follows. A gelator was dissolved in CH_2Cl_2 (0.3 g). To this solution were added a catalyst (acid or amine: see Table 2), solvent, TEOS and water in this order (also see Table 2 for their concentrations). The standard amounts of these components correspond to Run 1 in Table 2. The resultant solution was evaporated *in vacuo* until CH_2Cl_2 was removed (monitored by the mass decrease). When CH_2Cl_2 had been removed, the resultant solution gelled. This gel was sealed in a glass tube and left at 20 °C for 10 days. It was further heated at 200 °C for 1 h under an N_2 stream to complete the polymerization and to remove the residual stress evolved by shrinkage of the silica network. Finally, it was heated at 500 °C for 2 h under an N_2 stream and for 4 h in air for pyrolytic decomposition of the gelator.

Table 1 Gelation ability of **1** and **2**[a]

Solvent	**1**[b]	**2**
n-Hexane	G	I
Toluene	S	I
Dichloromethane	S	S
Chloroform	S	S
Diethyl ether	S	I
Tetrahydrofuran	S	I
Acetone	G	I
Methyl ethyl ketone	G	I
Acetonitrile	SG[c]	I
Methanol	SG[c]	G
Ethanol	SG[c]	G
Butan-1-ol	SG[c]	G
Octan-1-ol	G	G
Acetic acid	SG[c]	G
n-Propylamine	S	I
Diethylamine	S	I
Benzylamine	S	Gf[d]
TEOS	G	I
Water	I	I

[a]The solution (5 wt%) was warmed and then cooled to 4 °C to grow the gel: G = this gel was stable at room temperature, S = solution, I = insoluble. [b]Cited from refs. 16 and 21 [c]SG = The gel was formed at the concentration <1 wt%. [d]The gel was formed at 4 °C but turned into a solution at room temperature.

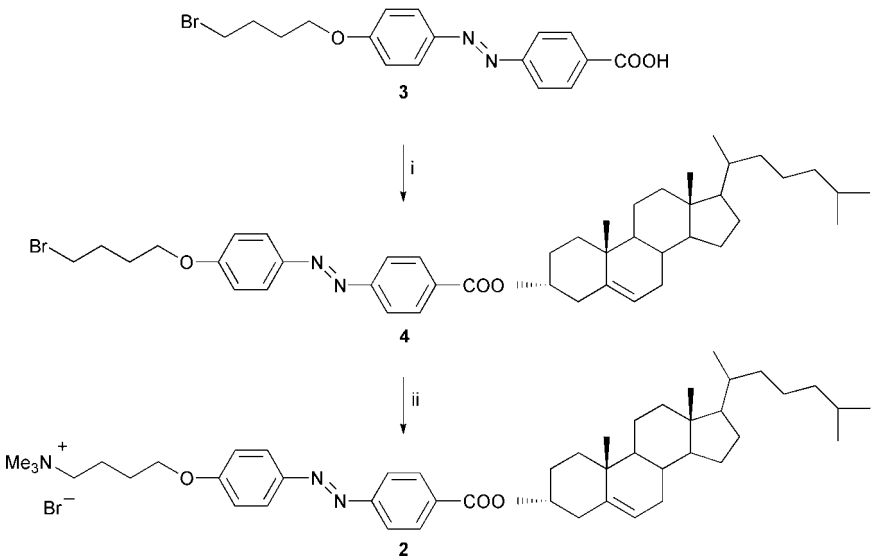

Scheme 1 *Reagents and conditions*: i, cholesterol, PPh_3, azodicarboxylic acid diethyl ester, THF, 20 °C, 18%; ii, NMe_3, THF, 20 °C, 69%.

Table 2 Influence of sol–gel polymerization conditions on the resultant silica structure[a]

Run	Catalyst	Solvent	Additive	Silica structure
1	$MeCO_2H$	$MeCO_2H$ (306 μL)	—	Hollow
2	$MeCO_2H$	$MeCO_2H$ (306 μL)	Me_4NCl (2.2 mg)	Hollow
3	$MeCO_3H$	$MeCO_2H$ (306 μL)	Me_4NCl (109.7 mg)	Granular
4	1.0 M HCl (15.6 μL)	$MeCO_2H$ (306 μL)	—	Granular
5	Benzylamine (5.7 μL)	Butan-1-ol (395 μL)	—	Hollow
6	Benzylamine (5.7 μL)	Octan-1-ol (346 μL)	—	Hollow

[a]**2** 5.0 mg (6.2×10^{-6} mol), TEOS 48.4 μL, and water 15.6 μL. Gelator **2** was added as a CH_2Cl_2 solution (0.3 g).

Instrumentation

A Hitachi S-4500 Scanning Electron Microscope was used for taking the scanning electron microscope (SEM) pictures. Samples were examined as grain mounts according to the conventional sample preparation and imaging techniques. For the observation of organogel fiber structures, a small piece of organogel was put in a flask and frozen in liquid nitrogen. The frozen specimen was evaporated by a vacuum pump for *ca.* 10 h. The accelerating voltage of SEM was 15 kV, and the emission current was 10 μm.

Transmission electron microscope (TEM) images were obtained on a Hitachi H7100 Transmission Electron Microscope operated at 100–125 kV. After silica samples were dispersed in hexane, they were spread on a carbon film of copper grids for TEM observation. Since the concentration of added sodium phosphotungstate is much lower than that of **2**, it scarcely affects the formation of organogel fiber structures. The organogel, which was prepared using sodium phosphotungstate instead of TEOS at **1** : **2** = 9 : 1 (mol/mol), was put on a copper grid and frozen in liquid nitrogen. The frozen specimen was evaporated by a vacuum pump for 10 h and examined according to the conventional imaging technique.

The nitrogen adsorption–desorption isotherm was measured on a Micromeritics ASAP-2000 apparatus. The pore size distribution was calculated from the desorption isotherm by the Barrett–Joyner–Halenda (BJH) analysis. The calcined sample was dehydrated by heating at 100 °C in flowing N_2 before the measurement.

Results and discussion

Gelation ability

One-dimensional stacking of a cholesterol moiety in **1** or **2** causes gelation, which is affected by the order of azobenzene and the absolute configuration of the C-3 in the cholesterol moiety. The gelation ability of newly synthesized **2** was tested using several organic solvents and compared with that of **1** (Table 1). It is seen from Table 1 that **2** is not very soluble in organic solvents but can gelate some solvents such as MeOH, EtOH, and $MeCO_2H$. Fig. 1 shows a TEM image of a freeze-dried gel prepared from $MeCO_2H$ (3.0 wt%) and stained with a 2 wt% sodium phosphotungstate solution. One can recognize well grown fibrils with diameters of 50–200 nm in this micrograph. As a gelator, however, **2** is not so versatile as **1**, because **1** can gelate 10 of 19 solvents and 5 of 10 gelated solvents are classified into SG whereas **2** gelates only 6 of 19 solvents and none of them is classified into SG. It is obvious that the trimethylammonium group is scarcely solvated in most organic solvents and therefore, the aggregate tends to separate from the solvent as the precipitate. Hence, this unfavorable functional group is introduced only to evaluate a hypothesis described below.

Creation of novel hollow fiber silica

It is known that compound **1** can gelate tetraethoxysilane (TEOS).[16,21] Firstly, TEOS in this gel was polymerized under acidic or basic reaction conditions. SEM observation indicated, however, that the resultant silica always showed the conventional granular structure and the new structure which might be constructed using these gelator fibrils as a template was not found at all. Presumably, TEOS polymerization proceeds randomly without any relation to the presence of these gelator fibrils or it destroys the fibrous organogel structure by compaction of voids in the network as a result of the TEOS hydrolysis and condensation. This system begins with the organogel phase and is terminated with the silica gel phase. These two phases are not compatible with each other. Thus, it is important for successful sol–gel transcription to maintain the organogel structure stably to "tame" TEOS polymerization. If TEOS polymerization proceeds according to its own preference, such transcription cannot take place. Hence, we newly synthesized compound **2** which bears a cationic quaternary ammonium group like conventional cationic surfactants generally used as templates for sol–gel polymerization. What we expected here is the electrostatic interaction between the propagating silica species and the cationic gelator fibrils: that is, the oligomeric silica should carry anionic charges, which can generate an adsorption driving force onto the cationic gelator fibril surface. Thus, sol–gel polymerization of TEOS was carried out in **2** + $MeCO_2H$ gel. In Fig. 2, two pictures are shown which are (a) an SEM picture of the silica gel and (b) a TEM picture of the silica gel obtained from **2** + $MeCO_2H$ gel. It is clearly seen from Fig. 2a that being different from the conventional granular silica obtained from **1** + $MeCO_2H$ gel, the organogel of **2** results in well grown fibrous silica and very interestingly, these fibers have a tubular structure with inner diameters of 10–200 nm (Fig. 2b). Although the silica may shrink to some extent during calcination, the size is nearly comparable with that of the gelator fibrils (50–200 nm: Fig. 1). This observation is further supported by the following sorption experiment. Fig. 3 shows the nitrogen adsorption–desorption isotherm to estimate the pore size distribution of this tubular silica after calcination. The pore size was calculated from the desorption isotherm by the Barrett–Joyner–Halenda (BJH) analysis. The results established that this silica sample has two specific pore sizes, 6 nm and 50 nm. As shown in Fig. 1, the size of the organogel fibers, which act as a template for sol–gel polymerization, has a wide distribution. This feature should be reflected by the wide distribution of both the inner and the

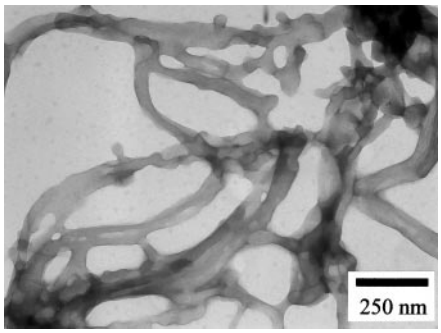

Fig. 1 TEM image for the xerogel of **2** + $MeCO_2H$ gel.

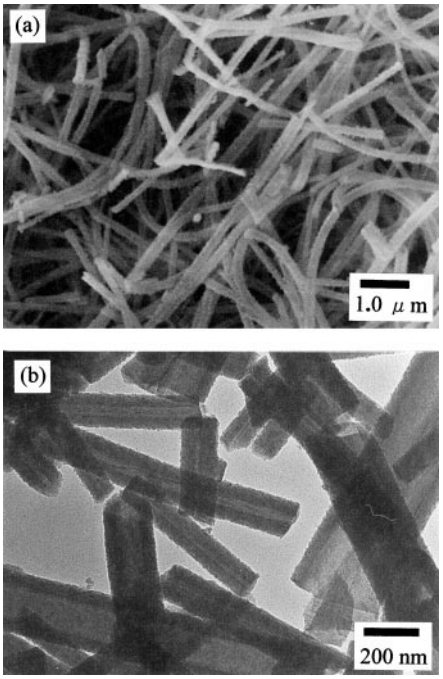

Fig. 2 SEM and TEM images ((a) and (b), respectively) for the silica obtained by sol–gel polymerization of TEOS in **2** + $MeCO_2H$ gel.

outer diameters in the resultant tubular silica. Judging from Fig. 2b, peaks around the 50 nm pore diameter are attributed to the inner diameter of the hollow fiber structure. On the other hand, the assignment of the 6 nm pore diameter is more difficult. Careful examination of Fig. 2a reveals that there are numerous micro silica particles on the surface of fibrous silica. These particles should be produced by polymerization after the fibrous structure has been constructed. Presumably, they result in the bumpy structure with *ca.* 6 nm crevices. The BET surface area and BJH pore volume were estimated to be 299 $m^2\ g^{-1}$ and 0.683 $cm^3\ g^{-1}$, respectively.

Here, we consider why **2** can act as the template while **1** cannot although both gelators aggregate into fibers in the organic solvents. When sol–gel polymerization is carried out in $MeCO_2H$, the propagation species is considered to be anionic.[26] Hence, the oligomeric silica species are adsorbed onto the cationic gelator fibrils owing to the electrostatic interaction and the polymerization further proceeds along these fibrils. This propagation mode provides a sort of organogel–silica gel composite fiber, which eventually yields a tubular structure after calcination (as schematically illustrated in Fig. 4). In contrast, the organogel fibrils of **1** without the cationic charge cannot adsorb the oligomeric silica species, so that the resultant silica showed only the conventional granular structure. Of course, similar granular silica was obtained by sol–gel polymerization in the absence of the gelator.

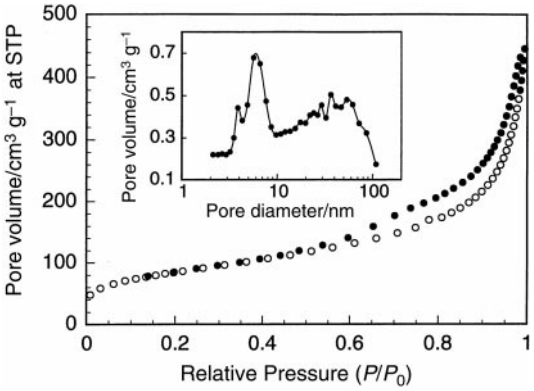

Fig. 3 Nitrogen adsorption–desorption isotherm and pore size distribution of the hollow fiber silica obtained from **2** + $MeCO_2H$ gel.

Sol–gel polymerization on the glass surface

To obtain further evidence that the organogel fibers really act as a template for the creation of the hollow fiber silica, we carried out sol–gel polymerization in a thin layer prepared on a glass plate. An acetic acid (306 μL) solution containing **2** (a small amount (0.3 g) of CH_2Cl_2 was used to dissolve this gelator), TEOS, and water (the same composition as that used for sol–gel polymerization) was spread on a glass plate immediately after the preparation (before the solution is gelated) and quickly evaporated to dryness under reduced pressure. As shown in the SEM image of Fig. 5a, one can recognize many fibrous assemblies. This implies that the fibers observed in Fig. 5a are identified to be those of **2** (as illustrated in Fig. 6a). This thin layer was left at 20 °C for 10 days in an atmosphere to allow sol–gel polymerization and then subjected to calcination. As shown in the SEM image of Fig. 5b, one can recognize many tubes, some of which feature an open, semicircular tube. This unique structure would be constructed by conversion of the organogel fibers (Fig. 6a) into the silica (Fig. 6c) *via* the organogel fiber–silica fiber composite (Fig. 6b). As expected, the diameters of the organogel fibers (*ca.* 100 nm) are comparable with the diameters of the silica nanotubes. These findings consistently support the view that the organogel fibers composed of **2** act as an efficient template to transcribe the organic aggregate superstructure into the inorganic silica material.

Importance of the electrostatic interaction

So far, we have assumed that the "anionic" TEOS oligomers are adsorbed by the electrostatic interaction onto the cationic organogel fibers to construct the tubular silica structure. To obtain unequivocal evidence for this rationale, sol–gel polymerization was carried out under the various reaction conditions. Run 1 is the standard condition which yields the tubular silica (Table 2). To this organogel was added tetramethylammonium chloride which is expected to suppress the specific electrostatic interaction. At 50 mmol dm^{-3} (2.2 mg

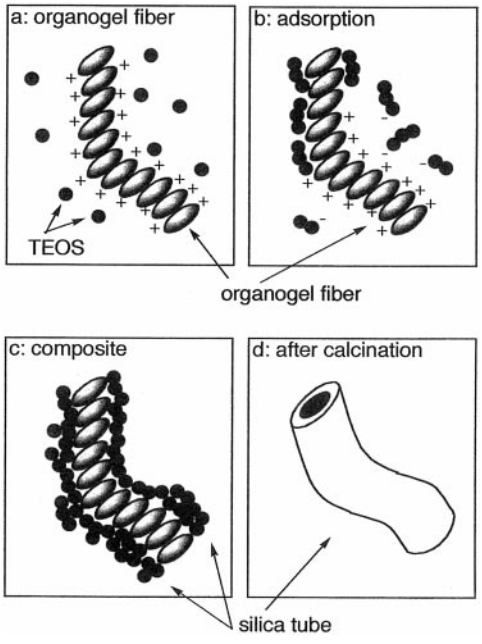

Fig. 4 Schematic representation of adsorption of anionic TEOS oligomers onto the cationic organogel fiber followed by creation of a hollow in the silica fiber by calcination.

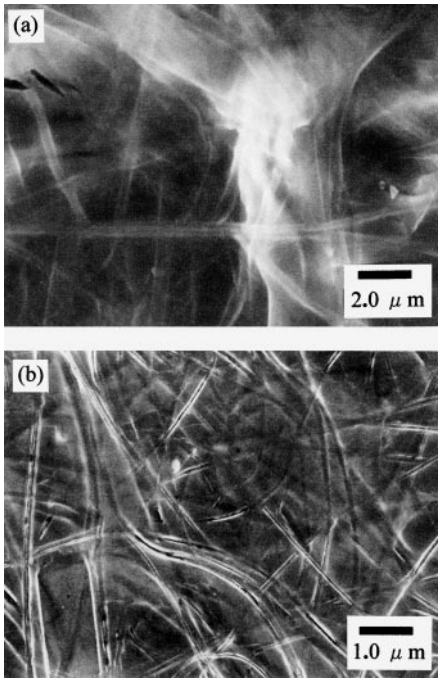

Fig. 5 (a) SEM image for the sol–gel polymerization solution (containing **2**) spread on the glass plate and quickly dried and (b) SEM image for the porous silica obtained on the glass plate.

in Run 2) the silica structure was scarcely affected, but when concentration was increased up to 2.7 mol dm^{-3} (109.7 mg in Run 3), the tubular structure disappeared and the conventional granular structure appeared. Since both solutions were gelated, it was supposed that an organogel fiber structure forms in them.

In the propagation process of TEOS, the isoelectric point is estimated to be 2.[26] This means that in pH regions lower than 2 the silica particles are no longer anionic. In Run 4, TEOS was polymerized in the organogel system using aqueous HCl as a

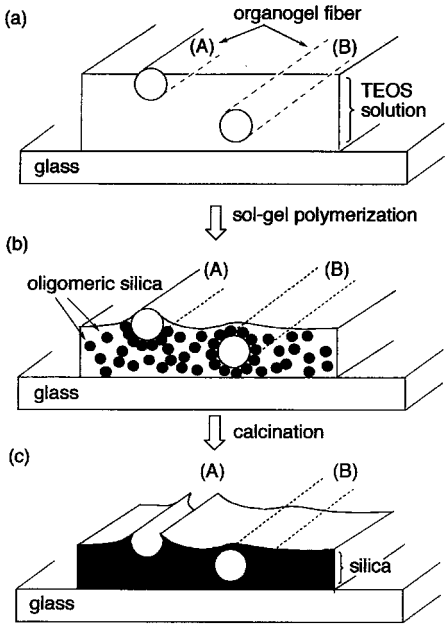

Fig. 6 Schematic representation of sol–gel polymerization in the organogel system spread on the glass plate: (a) the organogel fibers are formed, (b) sol–gel polymerization of TEOS proceeds to yield the organogel fiber–silica fiber composites, and (c) the porous silica is formed after calcination. (A) denotes an organogel fiber floating at the air–organogel interface which eventually results in a semicircular silica tube and (B) denotes an organogel fiber buried in the thin layer which eventually results in a silica tube.

catalyst. Although the TEOS polymerization was initiated to produce the silica particles, they were all granular under the SEM observation. Sol–gel polymerization was also carried out under the basic reaction conditions in butan-1-ol and octan-1-ol organogels using benzylamine as a catalyst (Runs 5 and 6). Under these "pH" conditions, the silanol groups are dissociated while the aggregates of **2** still carry the cationic charge of the quaternary ammonium groups. Hence, the electrostatic interaction operates very efficiently and the tubular silica results, as confirmed by the SEM observation.

The data obtained herein confirm that the electrostatic interaction plays an indispensable role in the creation of the novel tubular silica structure.

Accidental discovery of the novel "helical" silica

Primarily, we here tried to evaluate the influence of the "cationic charge density" on the creation of the tubular silica. The organogel fibers of cationic **2** can act as a template whereas that of neutral **1** cannot. This fact suggests that there exists a critical transition ratio of **1** : **2** from the tubular structure to the granular structure. When neutral **1** was mixed with cationic **2** (where the amount of **1** + **2** was kept constant: 2.48×10^{-6} mol; in addition, we confirmed that the organogel phase used for the sol–gel polymerization medium is still maintained at all **1** : **2** ratios), the hollow fiber silica still resulted at $R\,[= \mathbf{2}/(\mathbf{1}+\mathbf{2})] = 25$–100 mol% although the diameter size became gradually smaller (Fig. 7a) with increasing neutral **1** concentration. The result indicates that 25 mol% of the cationic

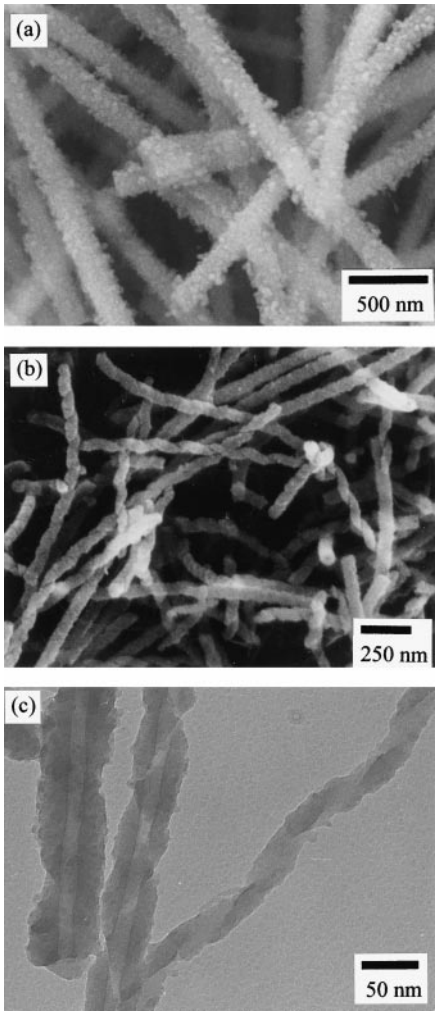

Fig. 7 SEM and TEM images of silica structures prepared using the mixture of **1** and **2** as a template: (a) SEM for $R = 25$ mol%, (b) SEM for $R = 10$ mol%, and (c) TEM for $R = 10$ mol%.

gelator is sufficient to adsorb the anionic silica particles onto the organogel fiber surface. Very surprisingly, the silica yielded at $R = 5 \approx 15$ mol% not only keeps the fibrous structure but possesses the right-handed helical structure (Fig. 7b). As shown in a TEM image in Fig. 7c, this helical silica also has a tubular structure with inner diameters of 10–15 nm, indicating that the organogel fibers act as a template to chirally arrange the adsorbed silica particles. However, one cannot clearly recognize the helical motif in the inner tube formed after calcination. At $R < 5$ mol%, the fibrous silica was no longer yielded and the resultant silica showed the conventional granular structure. The results indicate that the novel helical silica is obtained only under the very limited conditions of $R = 5$–15 mol%.

Careful examination of these SEM and TEM pictures reveals that (i) the observed helical silica fibers are all right-handed, (ii) the helical pitch is 100–200 nm, and (iii) the inner diameter (*ca.* 10 nm) shows a relatively narrow distribution. In particular, finding (i) supports the view that the helical structure results from the template effect of the "chiral" cholesterol-based gelators but not from the crystallization or shrinkage in the silica formation processes. Such non-template processes without any chiral element should yield both the right-handed and left-handed fibers in a 1 : 1 ratio, even if they are formed. Although a CD spectrum of the mixture of organogel and TEOS cannot be measured due to opacity induced by the formation of silica, the CD spectrum of the organogel at $R = 10$ mol% without TEOS clearly exhibits a positive sign for the first Cotton effect. This supports the view that the dipole moments of the gelator molecules are arranged in the right-handed helical orientation.

In Fig. 8, the diameter of the silica fibers is plotted against R. The silica fibers prepared from $R = 100$ mol% have a diameter of *ca.* 300 nm whereas they become smaller with the increase in the ratio of neutral **1**. At $R = 5 \approx 15$ mol% where the helical silica results, the outer diameter is only *ca.* 80 nm. The finding suggests that the organogel fibers with high R values have a strongly cationic surface and absorb many silica particles to make a thick silica wall, which eventually makes the fiber surface structure very vague. On the other hand, those with low R values adsorb only a small amount of silica particles to make a thin silica wall, which makes them more likely to be influenced by the organogel surface structure and to reproduce the organogel fiber structure accurately with the silica particles.

Provided that the helical silica is created as a result of transcription of the organogel fiber, one should find a similar helical motif in the organogel system. To find such a helical structure used as a template in the organogels we took a number of SEM and TEM pictures.[23] What we observed were mostly large bundles (*ca.* 100 nm diameter) without the helical higher-order structure.[23] Judging from the inner diameter of the helical silica (10–15 nm), it is inconceivable that they acted as the template for the transcription. We noticed that when the organogel is stained before the fibers grow up, many slender stripes appear in a gigantic bundle fiber.[23] The size of these stripes (*ca.* 10 nm) is comparable with that of the inner

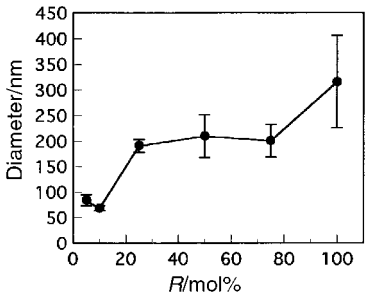

Fig. 8 Plot of the silica fiber diameter against R[= **2**/(**1** + **2**)].

diameter present in the helical silica fibers.[23] It thus occurred to us that if one can seize these incipient fibers before they aggregate into bundles, they would show the helical structure. With this expectation in mind, we diluted the standard sol–gel polymerization solution (see Table 2: here, $R = 10$ mol%) by 10-fold. When CH_2Cl_2 had been removed, the resultant solution only just gelled or looked like a slurry. Fig. 9 shows a TEM image of organogel fibers which was obtained from this diluted system. One can clearly recognize the fiber structure with a diameter of 10–20 nm and a helical pitch of 100–150 nm. These values are approximately consistent with the inner diameter and the helical pitch of the helical silica, respectively. One can thus propose that this helical motif of the oganogel fibers acts as a template for the creation of helical silica. This helical structure can be recognized by TEM for both the pre-staining (before the fibers grow up) or the post-staining (after the fibers grow up) conditions.

To obtain a further insight into the silica propagation mechanism we took TEM pictures as a function of polymerization time (Fig. 10). In order to slow down the polymerization velocity the TEOS concentration was reduced to 10% of the standard concentration (where $R = 10$ mol%). After 1 h, silica particles are scarcely adsorbed onto the organogel fibrils (Fig. 10a). At this stage, the helical structure of the organogel fiber can be still seen. With increasing polymerization time the fiber surface gradually becomes rough (Fig. 10b). Conceivably, the progress of sol–gel polymerization enforces the tight packing of silica particles and makes the silica fibers stiff. Under such tightly-packed conditions the most stable orientation which can relax the steric crowding would be a helical one and the twisting direction would be governed by the chirality in the cholesterol-based gel fibers. Finally, the novel helical silica structure appears (Fig. 10c). One may consider, therefore, that the helical silica structure is generated by accidental combination of several factors such as one-dimensional stacking of the cholesterol-based gelators, dilution of silica-adsorbing cationic sites, trapping of juvenile organogel fibers by adsorption of silica particles, and probably, helical arrangement of the cationic charges in the columnar aggregates.

To clarify the detailed transcription mechanism further discussions and experiments are still needed. It is undoubted at present, however, that the superstructure and the cationic charge in the organogel fibers play crucial and indispensable roles.

Conclusion

In conclusion, the present paper has demonstrated that organogels are applicable as a novel medium to the preparation of porous silica with tubular or helical structures.[27] In particular, the helical structure is characteristic of molecular assemblies which can be derived only from chiral "organic" materials. It is really surprising that such a higher-order

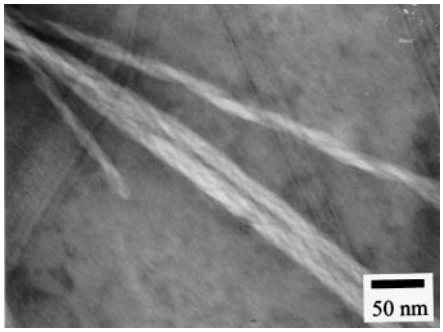

Fig. 9 TEM image of organogel fibers obtained at $R = 10$ mol% (stained by sodium phosphotungstate before the organogel fibers grow up).

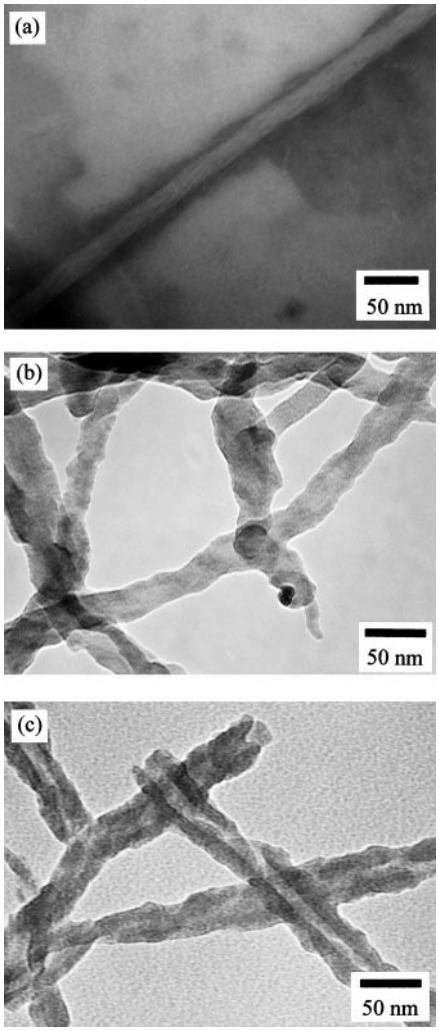

Fig. 10 Development of the helical hollow fiber structure with a reaction time: (a) 1 h, (b) 6 h, and (c) 3 days.

structure can be created even from "inorganic" materials. The key point of this unexpected finding is to transcribe the chirality present in the organogel fibers into silica utilizing electrostatic interactions. We believe that although such transcription is demonstrated here only for TEOS sol–gel polymerization, this concept is very essential and should be applicable to the creation of other "inorganic" materials formed *via* sol–gel polymerizations. For example, this system will be applicable to the asymmetric synthesis catalyzed by metals deposited on the helical silica. This system features that the asymmetric synthesis may be attained on the helical silica without any chiral "organic" source. Furthermore, high-temperature reactions, high recovery of catalysts, high turn-over numbers, *etc.* of the asymmetric synthesis may be also realized, which are very difficult to achieve with chiral "organic" catalysts.

Acknowledgements

We thank Mr M. Tanigawa and Ms T. Takebe for their helpful technical assistance.

References

1 T. Kunitake, Y. Okahata, M. Shimomura, S. Yasunami and K. Takarabe, *J. Am. Chem. Soc.*, 1981, **103**, 5401; T. Kunitake, *Angew. Chem., Int. Ed. Engl.*, 1992, **31**, 709.
2 C. T. Kresge, M. E. Leonowicz, W. J. Roth, J. C. Vartuli and J. S. Beck, *Nature*, 1992, **359**, 710; J. S. Beck, J. C. Vartuli, W. J. Roth, M. E. Leonowicz, C. T. Kresge, K. D. Schmitt, C. T-W. Chu, D. H. Olson, E. W. Sheppard, S. B. McCullen, J. B. Higgins and J. L. Schlenker, *J. Am. Chem. Soc.*, 1992, **114**, 10834.
3 S. S. Kim, W. Zhang and T. J. Pinnavaia, *Science*, 1998, **282**, 1302.
4 K. Sakata and T. Kunitake, *J. Chem. Soc., Chem. Commun.*, 1990, 504.
5 Q. Huo, D. I. Margolese, U. Ciesla, P. Feng, T. E. Gier, P. Sieger, R. Leon, P. M. Petroff, F. Schüth and G. D. Stucky, *Nature*, 1994, **368**, 317.
6 N. H. Mendelson, *Science*, 1992, **258**, 1633.
7 D. D. Archibald and S. Mann, *Nature*, 1993, **364**, 430; S. Barel and P. Schoen, *Chem. Mater.*, 1993, **5**, 145.
8 For related studies using racemic DL-tartaric acid, see H. Nakamura and Y. Matsui, *J. Am. Chem. Soc.*, 1995, **117**, 2651; F. Miyaji, S. A. Davis, J. P. H. Charmant and S. Mann, *Chem. Mater.*, 1999, **11**, 3021.
9 T. Asefa, M. J. MacLachlan, N. Coombs and G. A. Ozin, *Nature*, 1999, **402**, 867; J. Y. Ying, C. P. Mehnert and M. S. Wong, *Angew. Chem., Int. Ed.*, 1999, **38**, 56.
10 E. J. de Vries and R. M. Kellogg, *J. Chem. Soc., Chem. Commun.*, 1993, 238; M. de Loos, J. van Esch, I. Stokroos, R. M. Kellogg and B. L. Feringa, *J. Am. Chem. Soc.*, 1997, **119**, 12675; F. S. Schoonbeek, J. V. Esch, B. Wegewijs, D. B. A. Rep, M. P. Haas, T. M. Klapwijk, R. M. Kellogg and B. L. Feringa, *Angew. Chem., Int. Ed.*, 1999, **38**, 38; J. V. Esch, F. Schoonbeek, M. d. Loos, H. Kooijman, A. L. Spek, R. M. Kellogg and B. L. Feringa, *Chem. Eur. J.*, 1999, **5**, 937.
11 M. Aoki, K. Nakashima, H. Kawabata, S. Tsutsui and S. Shinkai, *J. Chem. Soc., Perkin Trans. 2*, 1993, 347.
12 K. Hanabusa, K. Okui, K. Karaki, T. Koyama and H. Shirai, *J. Chem. Soc., Chem. Commun.*, 1992, 1371; K. Hanabusa, A. Kawakami, M. Kimura and H. Shirai, *Chem. Lett.*, 1997, 191 and references therein.
13 J.-E. S. Sohna and F. Fages, *Chem. Commun.*, 1997, 327.
14 E. Otsuni, P. Kamaras and R. G. Weiss, *Angew. Chem., Int. Ed. Engl.*, 1996, **35**, 1324; L. Lu, T. M. Cocker, R. E. Bachman and R. G. Weiss, *Langmuir*, 2000, **16**, 20 and references therein; D. J. Abdallah and R. G. Weiss, *Langmuir*, 2000, **16**, 352; W. Gu, L. Lu, G. B. Chapman and R. G. Weiss, *Chem. Commun.*, 1997, 543; D. J. Abdallah and R. G. Weiss, *Chem. Mater.*, 1999, **11**, 2907; D. J. Abdallah and R. G. Weiss, *Chem. Mater.*, 2000, **12**, 406.
15 P. Terech, I. Furman and R. G. Weiss, *J. Phys. Chem.*, 1995, **99**, 9558 and references cited therein.
16 K. Murata, M. Aoki, T. Suzuki, T. Harada, H. Kawabata, T. Komori, F. Ohseto, K. Ueda and S. Shinkai, *J. Am. Chem. Soc.*, 1994, **116**, 6664 and references cited therein.
17 T. D. James, K. Murata, T. Harada, K. Ueda and S. Shinkai, *Chem. Lett.*, 1994, 273; J. H. Jung, Y. Ono and S. Shinkai, *Tetrahedron Lett.*, 2000, **40**, 8395.
18 S. W. Jeong, K. Murata and S. Shinkai, *Supramol. Sci.*, 1996, **3**, 83; J. H. Jung, Y. Ono and S. Shinkai, *Angew. Chem., Int. Ed.*, 2000, **39**, 1862.
19 T. Brotin, R. Utermöhlen, F. Fages, H. Bouas-Laurent and J.-P. Desvergne, *J. Chem. Soc., Chem. Commun.*, 1991, 416.
20 R. Wang, C. Geiger, L. Chen, B. Swanson and D. G. Whittern, *J Am. Chem. Soc.*, 2000, **122**, 2399; C. Geiger, M. Stanesch, L. H. Chen and D. G. Whittern, *Langmuir*, 1999, **15**, 2241.
21 For recent comprehensive reviews, see P. Terech and R. G. Weiss, *Chem. Rev.*, 1997, **97**, 3133; S. Shinkai and K. Murata, *J. Mater. Chem.*, 1998, **8**, 485; J. V. Esch. F. Schoonbeek, M. Deloos, R. Kellogg and B. L. Feringa, *Where It Is and Where It Is Going*, ed. R. Ungaro and E. Dalcanale, Kluwer, Dordrecht, 1999, p. 233.
22 K. Murata, PhD Thesis, Graduate School of Engineering, Kyushu University, 1997.
23 Preliminary communications: Y. Ono, K. Nakashima, M. Sano, Y. Kanekiyo, K. Inoue, J. Hojo and S. Shinkai, *Chem. Commun.*, 1998, 1477; Y. Ono, K. Nakashima, M. Sano, J. Hojo and S. Shinkai, *Chem. Lett.*, 1999, 1119. More recently, we found that the helical silica is also created by sol–gel transcription in chiral diaminocyclohexane-based organogel systems: J. H. Jung, Y. Ono, K. Hanabusa and S. Shinkai, *J. Am. Chem. Soc.*, 2000, **122**, 5008; J. H. Jung, Y. Ono and S. Shinkai, *Chem. Eur. J.*, 2000, **6**, 4552. In these systems, we could recognize not only the helical silica but also the granular silica. In the present system, most of the silica fibers in the SEM pictures show the helical structure (see Fig. 7).
24 N. Nakashima, K. Morimitsu and T. Kunitake, *Bull. Chem. Soc. Jpn.*, 1984, **57**, 3253.
25 A. Bose, B. Lal, W. A. Hoffmann and M. S. Manhas, *Tetrahedron Lett.*, 1973, 1619.
26 C. J. Brinker and G. W. Scherer, *Sol–Gel Science*, Academic Press, San Diego, 1990, 97.

27 Although a few inorganic materials with a helical structure were reported, they were not examples of the chiral template method as shown in this report. K. Robbie, M. J. Brett and A. Lakhtakia, *J. Vac. Sci. Technol.*, 1995, **A13**, 2991; Q. Huo, D. Zhao, J. Feng, K. Weston, S. K. Buratto, G. D. Stucky, S. Schacht and F. Schuth, *Adv. Mater.*, 1997, **9**, 974; H. Yang, N. Coombs and G. A. Ozin, *Nature*, 1997, **386**, 692; H. Yang, I. Sokolov, N. Coombs, C. T. Kresge and G. A. Ozin, *Adv. Mater.*, 1999, **11**, 1427; Y. Akiyama, F. Mizukami, Y. Kiyozumi, K. Maeda, H. Izutsu and K. Sakaguchi, *Angew. Chem., Int. Ed.*, 1999, **38**, 1420.